# The Effect of Microstructure on the Mechanical Properties of X80 Microalloyed Steel

Microalloyed steels are high-strength, low-alloy (HSLA) steels that are used primarily in the energy industries; more specifically, for pipeline applications,[1,2] tanks and penstocks.[3] These steels are able to achieve an excellent balance between strength and toughness through controlled alloying additions consisting of niobium, titanium and vanadium, and good weldability is maintained by keeping the carbon content very low. Mechanical properties are directly influenced by the microstructure (grain size, microconstituents, precipitate type and distribution, morphology, volume fraction and size fraction), which can be controlled and predicted through thermal mechanical controlled processing (TMCP).[4]

There is considerable interest in enhancing the work-hardening behavior in line pipe for strain-based pipeline designs. However, the effects of microstructure on the work-hardening characteristics of line pipe steels are not well known. Work performed by JFE Steel Corp. argues that high deformability can be achieved by introducing an on-line heat treatment system to interrupt phase transformation at a critical temperature. This heat-treatment on-line process (HOP) introduces an induction furnace that is situated directly between the accelerated cooling system and the hot leveler.[1] The accelerated cooling is interrupted at an intermediate temperature and the steel is reheated in the induction furnace before final cooling. This process allows for the simultaneous control of transformation, carbide precipitation and second phase formation while reducing the amount of scatter in mechanical properties in the through-thickness direction. As a result, the HOP improves mechanical performance, including tensile behavior (increasing yield and ultimate tensile strengths), hardness and work-hardening behavior, as compared with conventional TMCP conditions.[1,5] The current work applied a similar heat treatment to JFE's HOP in order to provide the groundwork for a subsequent investigation into the relationship between microstructure and work-hardening behavior. In this study, an interrupted thermal treatment (ITT) process was applied to an X80 microalloyed steel without straining. Efforts were focused on the development of different microstructures and the subsequent characterization of the various microconstituents without deformation; therefore, the effect of deformation on phase transformation and microstructural development was not included in this study.

A general "microstructure development map" was created with the intent of determining the effect of the following parameters on microstructure development: primary cooling rate, interrupt temperature, time at the interrupt temperature, reheat temperature, time at the reheat temperature and secondary cooling rate. Figure 1 shows the general microstructure


## Abstract

The aim of this study was to determine the relationship between microstructure and work-hardening characteristics of an X80 microalloyed steel. An interrupted thermal treatment process was applied to generate a variety of microstructures in various fractions and morphologies.


## Authors


K. Jonsson
M.Sc. candidate, University of Alberta, Edmonton, Alta., Canada
kjonsson@ualberta.ca



D. Ivey
professor of materials engineering, director, Alberta Centre for Surface Engineering and Science (ACSES), University of Alberta, Edmonton, Alta., Canada



H. Henein
professor of materials engineering, University of Alberta, Edmonton, Alta., Canada



S. Nafisi
research engineer, EVRAZ Inc. NA, Regina, Sask., Canada
shahrooz.nafisi@evrazincna.com

L.E. Collins
director of research, Research and Development Center, EVRAZ Inc. NA, Regina, Sask., Canada

Figure 1

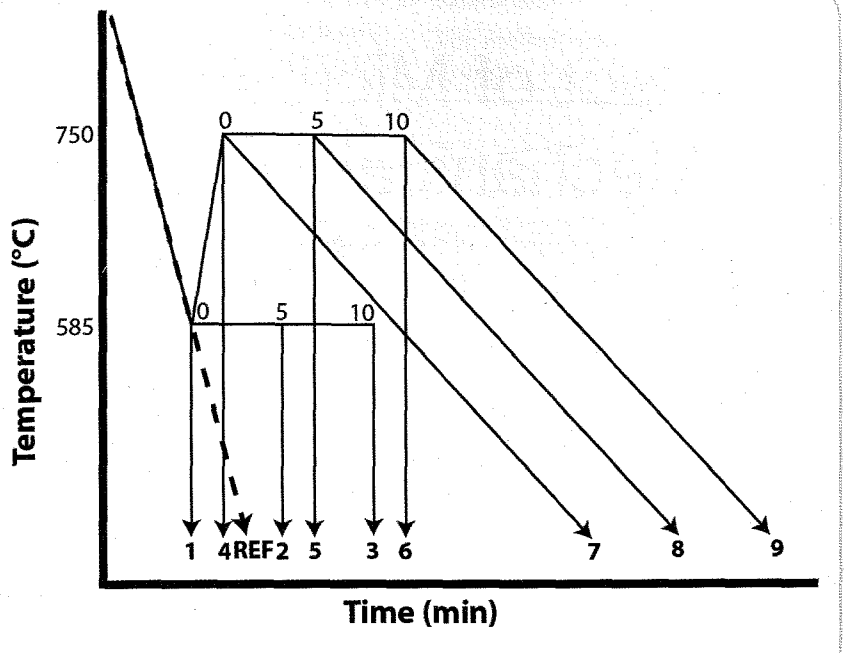


Schematic outline of the "microstructure development map" at various stages in the interrupted thermal treatment (ITT) process.

development map that will be discussed in this paper. The only parameters that were varied were the hold time at the interrupt temperature, hold time at the reheat temperature and secondary cooling rate. The other variables (primary cooling rate, interrupt temperature and reheat temperature) were kept constant in order to directly compare the effect of hold times at the two temperatures and the effect of secondary cooling rate on microstructure development. The reference sample shown in Figure 1 was continuously cooled at 10°C/second to represent a cooling rate that is easily attained in steel production.

## Experimental Procedure

Table 1 details the complete thermal history employed for each sample discussed in this study. For simplicity and consistency, all samples were austenitized at the same temperature (945°C) for the same amount of time (5 minutes). The chemical composition of the X80 steel is as follows: 0.06 wt. % carbon, 1.7 wt. % manganese, 0.3 wt. % molybdenum, 0.3 wt. % silicon and <0.2 wt. % combined of chromium, vanadium, niobium and titanium. The X80 steel samples were obtained from as-rolled plate that was subjected to standard TMCP techniques according

Table 1

**Thermal History of ITT Samples**

| Sample ID | Primary cooling rate (°C/second) | Interrupt temperature (°C) | Hold time (minutes) | Reheat temperature (RT) (°C) | Hold time (minutes) | Secondary cooling rate (°C/second) |
|---|---|---|---|---|---|---|
| REF | 10 | — | — | — | — | — |
| 1 | 10 | 585 | 0 | — | — | quench to RT |
| 2 | 10 | 585 | 5 | — | — | quench to RT |
| 3 | 10 | 585 | 10 | — | — | quench to RT |
| 4 | 10 | 585 | 0 | 750 | 0 | quench to RT |
| 5 | 10 | 585 | 0 | 750 | 5 | quench to RT |
| 6 | 10 | 585 | 0 | 750 | 10 | quench to RT |
| 7 | 10 | 585 | 0 | 750 | 0 | 3 |
| 8 | 10 | 585 | 0 | 750 | 5 | 3 |
| 9 | 10 | 585 | 0 | 750 | 10 | 3 |

Figure 2

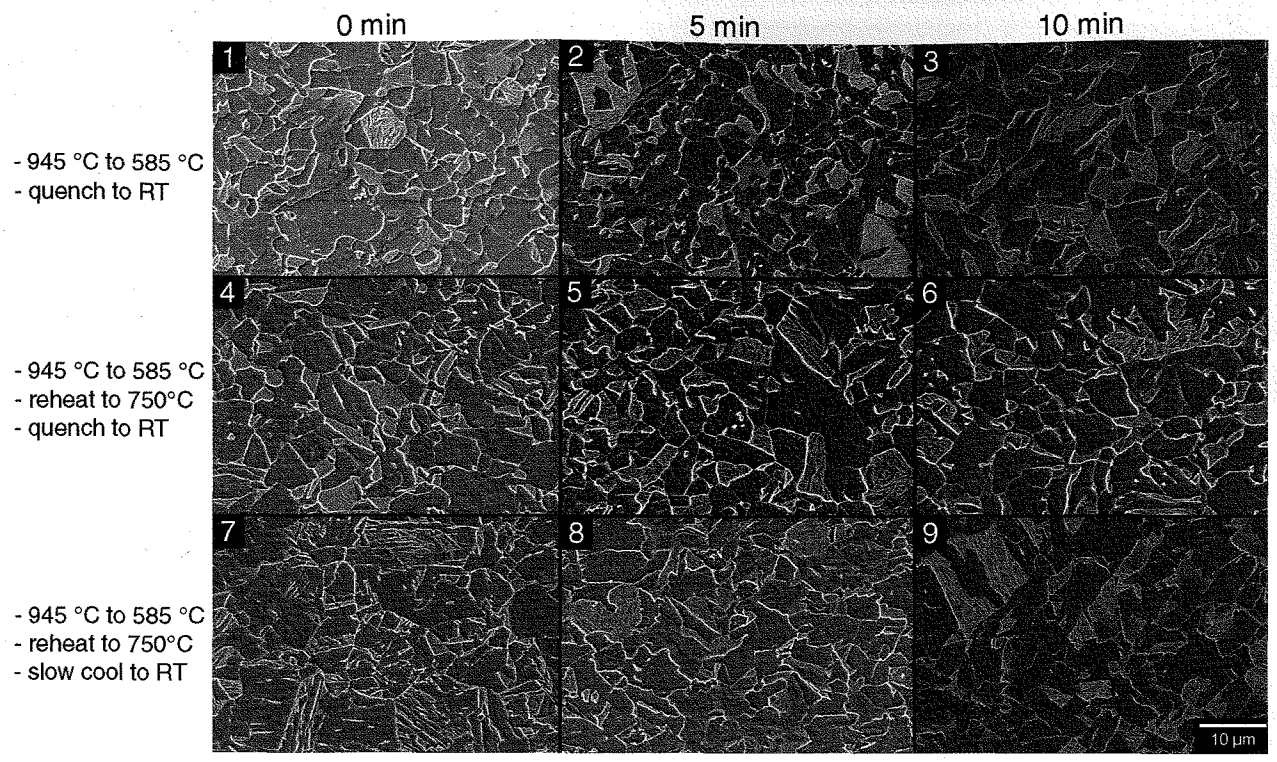


SEM SE images of ITT trial samples labeled according to Table 1.

to the designated operating conditions. The samples were machined into 80-mm-long cylindrical bars with a uniform diameter of 10 mm for subsequent thermal cycling in a Gleeble 3800 machine. The ITT samples were cut using a horizontal band saw into smaller (30-mm) pieces that contained the area subjected to the thermal treatment in the Gleeble. They were subsequently cut in half lengthwise using a diamond blade in order to access the centerline. The samples were mounted in Bakelite using a hot press and then ground using progressively finer silicon carbide grit papers; more specifically, 120, 320, 400, 600 and 800 grit size. Final polishing was conducted using 1-µm diamond paste followed by 0.05-µm alumina slurry. The samples were etched using 2% Nital for approximately 5 seconds to expose the microstructural features. Scanning electron microscope (SEM) images were obtained using a Philips XL30 SEM operated at 10 kV. A JEOL JEM 2010 transmission electron microscope (TEM), operated at 200 kV, was also used to examine selected features at higher resolution. A focused ion beam instrument (Hitachi NB5000, dual beam focused ion beam (FIB)/SEM) was used to fabricate site-specific TEM samples. Hardness measurements were obtained from a Mitutoyo MVK-H1 hardness testing machine using a 100 g load.

## Results and Discussion

Figure 2 shows SEM secondary electron (SE) micrographs for each ITT sample as labeled in Table 1; the reference sample is shown in Figure 3. The samples consist mostly of darker regions (ferrite) and lighter regions (referred to here as bainitic ferrite). The bainitic ferrite is characterized by angular, jagged grains, whereas the ferrite appears flat and relatively equiaxed. The reference sample is largely dominated by ferrite grains, as shown in Figure 3. Since ferrite is a softer phase than bainitic ferrite, ferrite etches more readily and, as a result, appears recessed in an oblique SEM SE image, as shown in Figure 3. The bainitic ferrite grains in the reference sample are small and do not reveal a complex or lath-like internal structure, whereas the morphology of bainitic ferrite in the ITT trial samples shows a more noticeable internal structure and distinct laths within the grains.

The microconstituents observed in the SE SEM micrographs for samples 1, 2 and 3 are very similar in phase fraction and morphology, which indicates that there is no significant effect of hold time at the interrupt temperature on the final microstructure. Similarly, no significant difference in morphology of the ferrite and bainitic ferrite phases is observed for samples 4, 5 and 6. Samples 7, 8 and 9 reveal that the hold time at the reheat temperature results in a more homogeneous microstructure and larger ferrite grains. Sample 9 has more ferrite than samples 7 and 8, which may be attributed to the significant amount of time at the reheat temperature (RT) and the subsequent slow cooling rate to room temperature. In order to determine the effect of secondary cooling rate on microstructural development, one can compare the

Figure 3

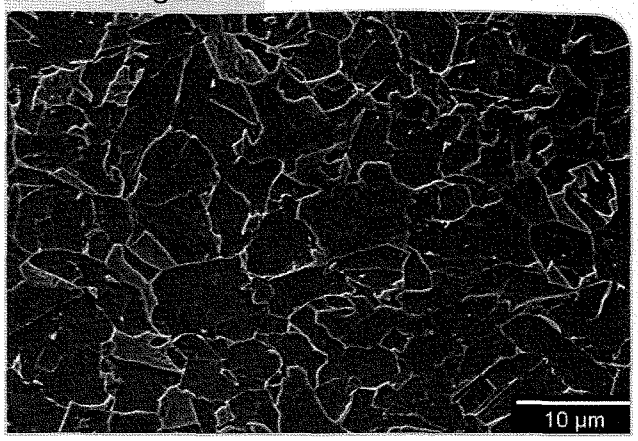


SEM SE images of reference sample (continuously cooled from 945°C to room temperature at 10°C/second).

micrographs in the second and third rows of Figure 2. When evaluating the micrographs for samples 4 and 7 in Figure 2, the morphology of bainitic ferrite in sample 7 is more jagged and irregular than sample 4. The same trend is observed for the full ITT samples held at the reheat temperature for 5 and 10 minutes (samples 8 and 9) — the bainitic ferrite appears more angular in samples 8 and 9 as compared with samples 5 and 6.

In order to accurately identify the phases present in these microstructures, TEM samples were prepared using the focused ion beam (FIB) technique. Specific regions of interest were identified in the SEM, and then a small section (approximately 10 µm long x 2 µm wide x 10 µm deep) was "plucked" from the sample and subsequently milled with gallium ions to electron transparency in the width direction. Two TEM samples were fabricated using this technique: one grain from sample 1 (originally thought to be pearlite, due to the lamellar-like internal structure) and one grain from sample 2 (initially classified as bainitic ferrite). Figure 4 shows the "pearlite-like" grain that was analyzed both in the general overall microstructure (Figure 4a) and the specific region that was examined in the TEM (Figure 4b). Figure 5 shows TEM images from the FIB sample at various magnifications. Figure 5a is a low-magnification bright field (BF) image of the entire sample, while Figure 5b shows a higher-magnification BF image of the region indicated in Figure 5a. The region of interest (Figures 4a and 4b) has a lath-like structure, as shown in Figure 5b. The individual laths exhibit different contrast due to slight orientation differences. Laths that appear darker (labeled as 1 and 2 in Figure 5b) are oriented closer to the Bragg condition and, as such, diffract more strongly than the laths that are oriented farther from the Bragg condition (spot 3). As a result, the selected area diffraction (SAD) patterns that were taken from these adjacent laths (labeled as 1–3 in Figure 5b) have different brightness levels, as observed in Figures 5c–e. The SAD patterns for laths 1–3 are similar and the patterns were indexed to ferrite with zone axes close to a [012] orientation. The slight misorientation among the laths is indicative of a bainitic structure and not a pearlitic one. Furthermore, no iron carbide precipitates were identified in this sample, which would have been present in a pearlite grain. As a result, this grain was identified as bainitic ferrite.

The second region that was investigated in the TEM was from sample 2, and both the overall microstructure (Figure 6a) and the specific region that were examined in the TEM (Figure 6b) are shown. Figure 7a shows a low-magnification TEM micrograph

Figure 4

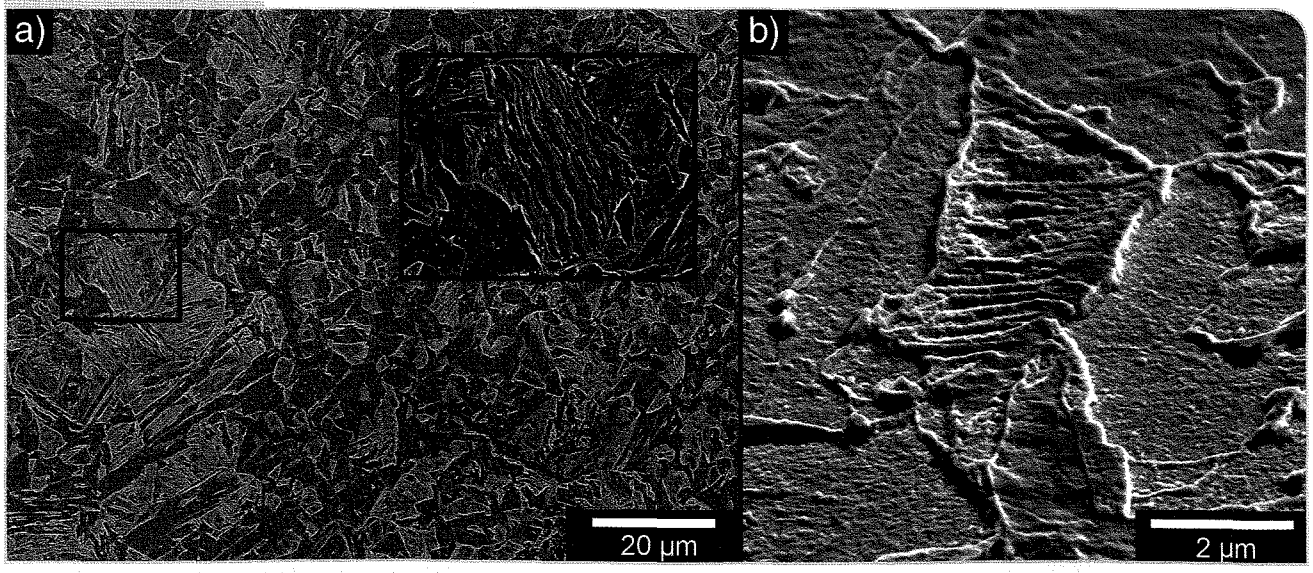


SEM SE images of "pearlite-like" grain from sample 1: (a) SEM SE image with "pearlite-like" grain identified in inset, and (b) region from which FIB sample was prepared for TEM analysis.

Figure 5

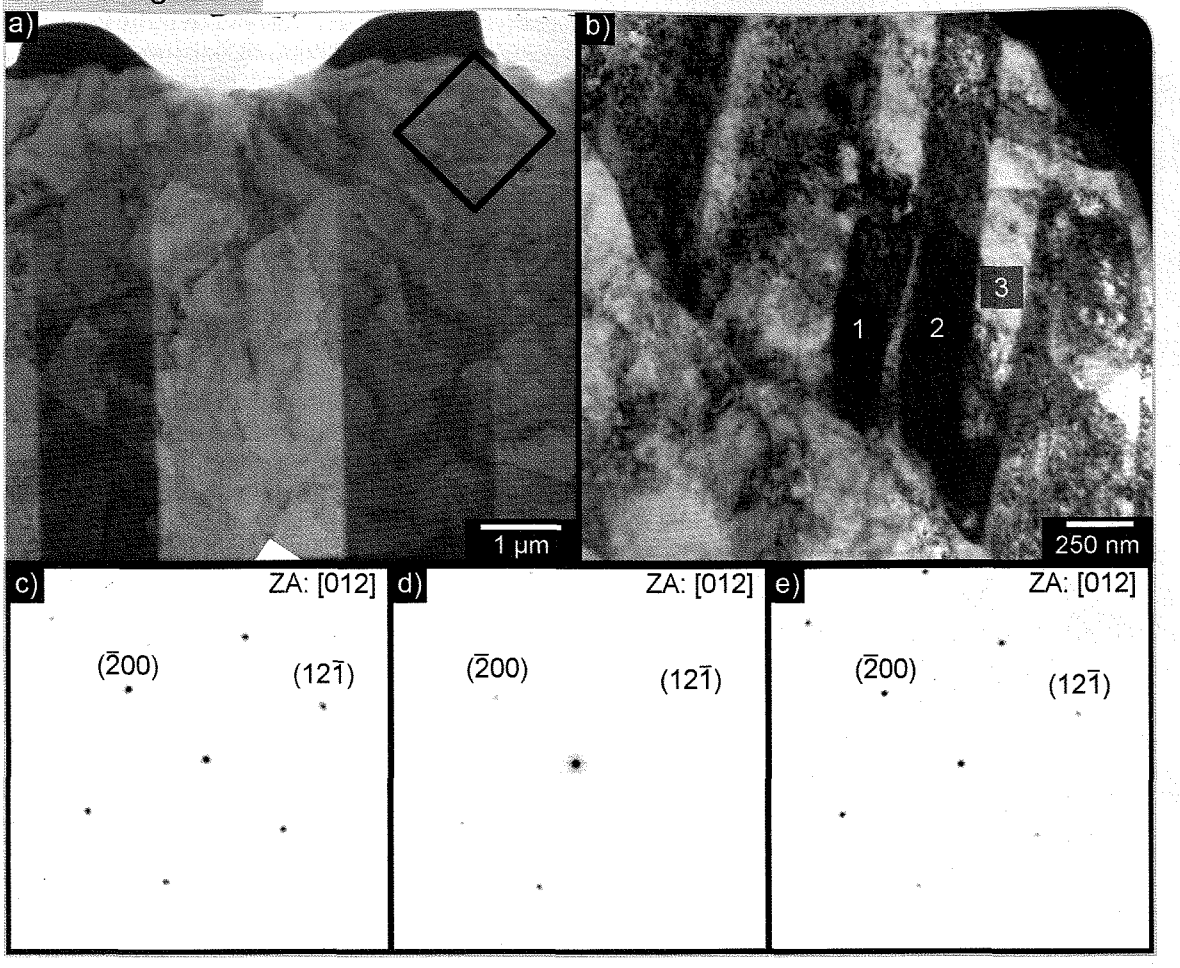


TEM BF images and SAD patterns of FIB sample fabricated from region in Figure 4: (a) low-magnification image; (b) higher-magnification image tilted to reveal diffraction contrast arising from the grain substructure with laths indicated; and (c), (d) and (e) SAD patterns from the laths indicated in (b).

Figure 6

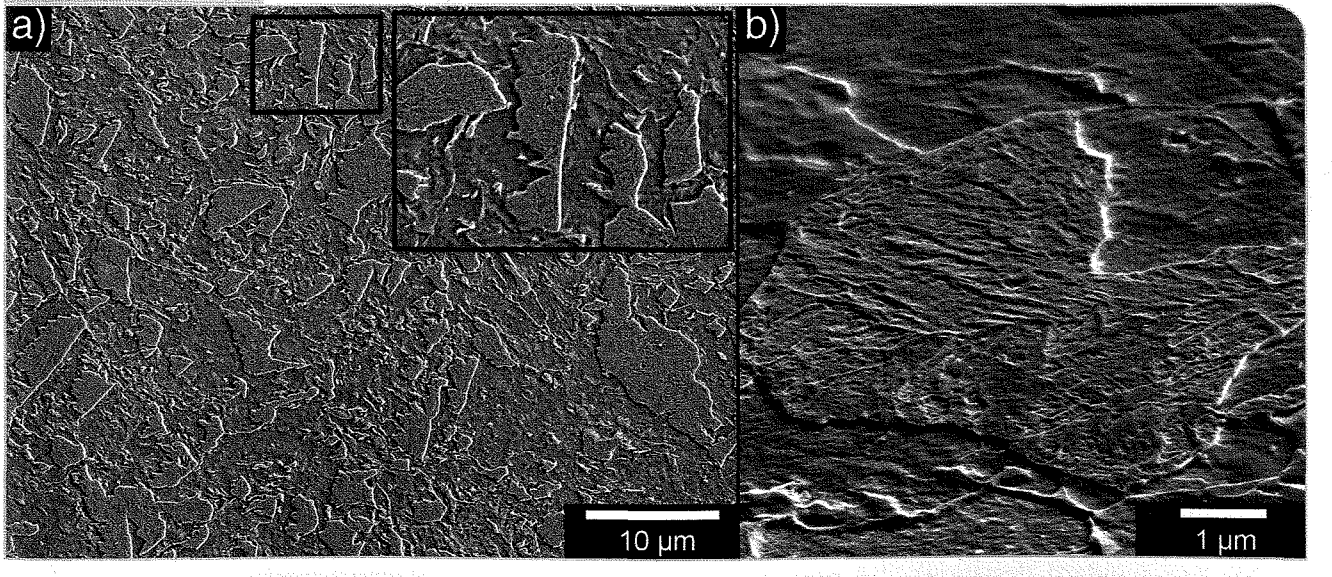


SEM SE images of "bainite-like" grain from sample 2: (a) SEM SE image with "bainite-like" grain identified in inset, and (b) region from which FIB sample was prepared for TEM analysis.

Figure 7

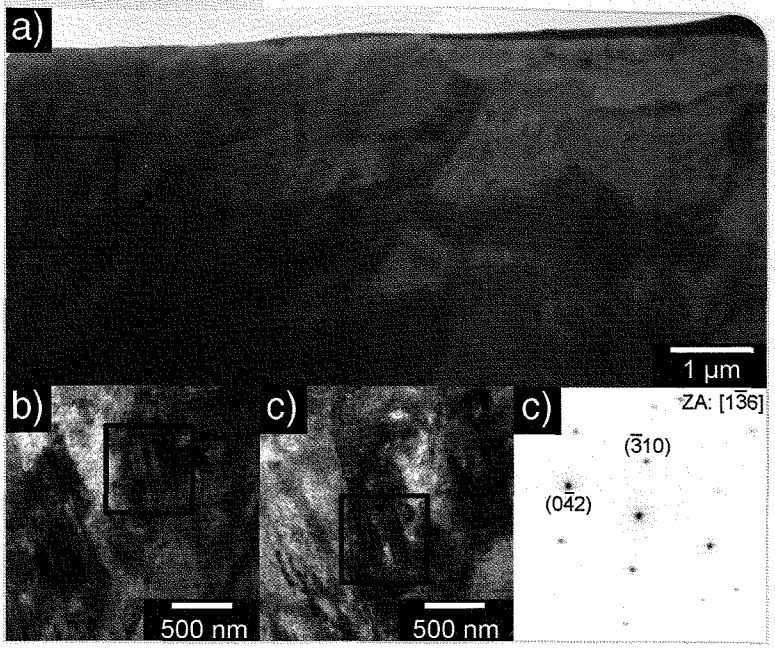


TEM BF images and SAD pattern of FIB sample fabricated from region in Figure 6b: (a) low-magnification image; (b) and (c) higher-magnification images of region indicated in (a), tilted at different angles to reveal diffraction contrast arising from microtwins; and (d) SAD pattern from region indicated in (b).

with a higher-magnification image in Figure 7b. Figure 7c is the same region as Figure 7b, but taken at a different tilt angle to illustrate that the microstructural features (in this case, microtwins) go in and out of contrast as the tilt angle is changed. Figure 7b was taken at a tilt angle of −4.2° and Figure 7c was tilted to an angle of −17.6°. The SAD pattern shown in Figure 7d, from the region indicated in Figure 7b, can be indexed to ferrite with a zone axis close to a [1$\bar{3}$6] orientation. However, since the c/a ratio for martensite is very close to 1 for steels with this low carbon content, the presence of the microtwins confirms that the phase is, in fact, martensite.

The measured hardness values are shown in Table 2. The hardness values represent the arithmetic average of five indents taken across the sample surface. The reference sample provides the baseline for all subsequent hardness values and corresponds to the lowest hardness value of 222.8 HV. Since bainitic ferrite has the highest hardness value of the microconstituents (after martensite), it would be expected that the hardness values for samples 1, 2 and 3 would be the highest. This is due to the quench treatment that the samples underwent after the hold at the intermediate temperature, which resulted in the formation of martensite or fine bainitic ferrite. Sample 1 had the highest hardness value of all ITT samples; the hardness is almost 37 HV higher than the reference sample and also significantly higher than both samples 2 and 3. Samples 2 and 3 had almost identical hardness values (within one standard deviation) and were approximately 8 HV higher than the reference sample. The negative trend in hardness as hold time at 585°C increases indicates that the isothermal hold is detrimental to hardness.

Comparing samples 4, 5 and 6 (samples that were cooled to the interrupt temperature then reheated to the reheat temperature and held for 0, 5 or 10 minutes before quenching to room temperature), the sample with the highest hardness is sample 6, which had a 10-minute hold time at the reheat temperature. Sample 6 also had the second highest hardness value of all the ITT samples. Sample 4 has the lowest hardness value of the three samples, and is almost identical to the reference sample. Sample 5 had a hardness value that was in between samples 4 and 6, and was 11 HV higher than the reference sample. As hold time increases at the reheat temperature of 750°C, the hardness value increases. This may occur because the primary phase that forms at 585°C is re-austenitized at 750°C, and the austenite then transforms to a very hard phase upon quenching. The 10-minute hold at 750°C allows for more transformation than the 5- and 0-minute holds and, as a result, yields a higher hardness than the other two samples.

The samples that underwent the complete ITT process (samples 7, 8 and 9) showed a negative trend in hardness with increasing hold time. The microstructure for sample 7 in Figure 2 has a significant amount of bainitic ferrite and also corresponds to the highest hardness in this set of samples. Samples 8 and 9 have more ferrite grains than that observed for sample 7, and have much lower hardness values than sample 7. The negative correlation between hardness and hold time at the reheat temperature can be explained by considering the effect of secondary cooling rate. Samples 4, 5 and 6 showed that increasing the hold time at 750°C caused an increase in hardness, which can be

Table 2

**Vickers Hardness Data (HV) for ITT Samples**

| Sample | Average hardness (HV) | Hardness relative to REF |
|---|---|---|
| REF | 222.8 ± 3.3 | — |
| 1 | 259.6 ± 3.6 | 36.8 |
| 2 | 232.4 ± 2.8 | 9.6 |
| 3 | 230.1 ± 3.4 | 7.3 |
| 4 | 224.5 ± 4.8 | 1.7 |
| 5 | 233.6 ± 2.2 | 10.8 |
| 6 | 248.7 ± 1.7 | 25.9 |
| 7 | 240.7 ± 2.7 | 17.9 |
| 8 | 233.6 ± 3.1 | 10.8 |
| 9 | 233.3 ± 3.2 | 10.5 |

attributed to the re-austenitization of the primary structure formed at 585°C and then the subsequent formation of a hard phase during the quenching process. For samples 7, 8 and 9, the hold time at 750°C causes the same austenitization process as in samples 4, 5 and 6; however, the cooling rate for samples 7, 8 and 9 is significantly slower and thus promotes ferrite formation instead of the hard phase that results from the quenching process in samples 4, 5 and 6. Since ferrite is a soft phase, the hardness for the slow-cooled samples should be lower than the quenched samples and, furthermore, the longer hold times at the reheat temperature should also promote more ferrite production and thus lower hardness values as well.

As mentioned earlier, the HOP treatment applied by JFE Steel is performed to improve mechanical behavior; more specifically, work-hardening behavior. Although tensile tests were not obtained for these samples, the hardness tests provide an indication of mechanical performance. The results from this study show that the ITT process marginally enhanced the hardness values, as samples 7, 8 and 9 showed a minimal improvement of approximately 11 HV relative to the reference sample. As mentioned earlier, the ITT samples were thermally treated under conditions of no strain. As a result, the microstructures that formed during heat treatment could be substantially different than what would occur under severe deformation (such as in a steel mill), since strain-induced precipitation and phase transformation do not occur and the strengthening effect from dislocations is not observed.

## Conclusions

An X80 steel was subjected to different interrupted thermal treatment (ITT) schedules, which involved applying various heating and cooling schedules to generate a range of microstructures. Samples were austenitized and then cooled to an interrupt temperature of 585°C (held for up to 10 minutes), followed by either quenching to room temperature or reheating to an intermediate temperature of 750°C (held for up to 10 minutes). The reheated samples were either quenched or cooled at a slow rate. The following conclusions can be made regarding the evidence presented in this study:

1. The microstructures for the ITT samples were predominantly bainitic ferrite and ferrite with a few isolated grains of martensite. The morphology of the bainitic ferrite grains was angular and jagged, whereas the ferrite grains were relatively equiaxed.
2. Varying the hold time at the interrupt temperature did not have a significant effect on microstructure development, although the hardness was significantly affected. A 0-minute hold time resulted in a hardness that was 37 HV higher than the reference sample, whereas a 5- and 10-minute hold only marginally improved the hardness relative to the reference sample.
3. Increasing the hold time at the reheat temperature did not substantially affect the final microstructure for the quenched samples, but the samples that were slow cooled had higher ferrite content as the hold time at the reheat temperature was increased.
4. The hardness values for the reheated and quenched samples showed a positive trend with hold time: the 0-minute hold sample had a hardness value that was almost identical to the reference sample, whereas a 10-minute hold resulted in an improvement of 26 HV relative to the reference sample. This trend may be attributed to transformation to austenite at 750°C. A longer hold time at the reheat temperature results in more austenite that is subsequently transformed to a hard phase upon quenching.
5. The samples that were subjected to the full ITT process had a decrease in hardness as hold time at 750°C was increased; however, the hardness values were at least 10 HV higher than the reference sample. The decrease in hardness as a function of increasing hold time can be attributed to the increased amount of ferrite that forms during slow cooling after heat treatment at 750°C.

## Acknowledgments

This work was supported by EVRAZ Inc. NA and the Natural Sciences and Engineering Research Council of Canada. The authors would like to thank M. Kupsta (National Research Council of Canada's National Institute for Nanotechnology) for his assistance with the FIB sample preparation and L. Good from EVRAZ Inc. NA Research for performing Gleeble tests.

## References

1. J. Kondo, et al., "High Performance UOE Linepipes," *JFE Technical Report,* Vol. 7, 2006, pp. 20–26.

2. A. Fujibayashi and K. Omata, "JFE Steel's Advanced Manufacturing Technologies for High Performance Steel Plates," *JFE Technical Report,* Vol. 5, 2005, pp. 10–15.

3. K. Araki, et al., "High Performance Steel Plates for Tank and Pressure Vessel Use — High Strength Steel Plates With Excellent Weldability and Superior Toughness for the Energy Industry," *JFE Technical Report,* Vol. 5, 2005, pp. 66–73.

4. D.J. Colvin, et al., Austenite Decomposition During Continuous Cooling of an HSLF-80 Plate Steel," *Metallurgical and Materials Transactions A,* Vol. 27A, 1996, pp. 1567–1571.

5. O. Mitsuhiro, et al., "Development of a High-Deformability Linepipe With Resistance to Strain-Aged Hardening by HOP (Heat-Treatment On-Line Process)," *JFE Technical Report,* Vol. 12, 2008, pp. 8–14. ✦



This paper was presented at MS&T'11 — The Materials Science & Technology Conference and Exposition, Columbus, Ohio, and published in the Conference Proceedings.